Published OnlineFirst March 10, 2009; DOI: 10.1158/0008-5472.CAN-08-3222

Research Article

CDC25B Mediates Rapamycin-Induced Oncogenic Responses in Cancer Cells

Run-qiang Chen,[1] Qing-kai Yang,[1] Bing-wen Lu,[2] Wei Yi,[1] Greg Cantin,[2] Yan-ling Chen,[1] Colleen Fearns,[3] John R. Yates III,[2] and Jiing-Dwan Lee[1]

Departments of [1]Immunology and Microbial Science, [2]Chemical Physiology, and [3]Chemistry, The Scripps Research Institute, La Jolla, California

Abstract

Because the mammalian target of rapamycin (mTOR) pathway is commonly deregulated in human cancer, mTOR inhibitors, rapamycin and its derivatives, are being actively tested in cancer clinical trials. Clinical updates indicate that the anticancer effect of these drugs is limited, perhaps due to rapamycin-dependent induction of oncogenic cascades by an as yet unclear mechanism. As such, we investigated rapamycin-dependent phosphoproteomics and discovered that 250 phosphosites in 161 cellular proteins were sensitive to rapamycin. Among these, rapamycin regulated four kinases and four phosphatases. A siRNA-dependent screen of these proteins showed that AKT induction by rapamycin was attenuated by depleting cellular CDC25B phosphatase. Rapamycin induces the phosphorylation of CDC25B at Serine375, and mutating this site to Alanine substantially reduced CDC25B phosphatase activity. Additionally, expression of CDC25B (S375A) inhibited the AKT activation by rapamycin, indicating that phosphorylation of CDC25B is critical for CDC25B activity and its ability to transduce rapamycin-induced oncogenic AKT activity. Importantly, we also found that CDC25B depletion in various cancer cell lines enhanced the anticancer effect of rapamycin. Together, using rapamycin phosphoproteomics, we not only advance the global mechanistic understanding of the action of rapamycin but also show that CDC25B may serve as a drug target for improving mTOR-targeted cancer therapies. [Cancer Res 2009;69(6):2663–8]

Introduction

Mammalian target of rapamycin (mTOR) is a cellular 289 kDa protein mediating signals derived from both growth factors and nutrients and is known to regulate cell growth, proliferation, and survival through controlling mRNA translation, metabolism, ribosome biogenesis, and autophagy (1–3). The mTOR pathway is commonly deregulated in human cancer. For example, in human breast cancer, mTOR is commonly deregulated by loss of PTEN (30% of human breast tumor; ref. 4), by mutation of PI3KCA (18–26%; ref. 4), and by overexpression of Her2 (15–30%; ref. 5): all of which are associated with a poor prognosis for breast cancer patients (5–7). Similarly, in human prostate cancer, mTOR is commonly deregulated by genetic aberrations such as low expression of PTEN, increased PI3K activity, and increased expression or activation of AKT in advanced prostate cancer (8–10). These aberrations also are indicators of a poor prognosis for prostate cancer patients (11, 12). More importantly, long-term androgen deprivation treatment for prostate cancer patients that reinforces the PI3K/AKT pathway also up-regulates mTOR activation in prostate tumor (9, 10). These abovementioned experimental and clinical data lead to the supposition that mTOR inhibitors (rapamycin and its derivatives) should be effective in treating human cancer. Unfortunately, recent clinical data indicates that rapamycin shows therapeutic potential in only few types of human cancer: endometrial carcinoma, renal cell carcinoma, and mantle cell lymphoma (13). These results could be explained by recent findings that mTOR inhibition by rapamycin phosphorylates and activates the oncogenic AKT and elF4E pathways while still suppressing the phosphorylation of p70S6K and 4E-BP1 (14) in cancer cells. However, the detailed molecular mechanisms regulating this rapamycin-dependent activation of oncogenic cascades are not clear. Progress toward understanding the underlying mechanisms is hindered by the limited number of known cellular targets for rapamycin. We recently improved the methodology for profiling the cellular phosphoproteome (15) and, using this technology, simultaneously profiled 6,179 phosphosites in cancer cells and identified 161 cellular proteins sensitive to rapamycin. Within these proteins, there are four kinases and four phosphatases, key mediators for cell signaling. We screened these proteins and found that depletion of cellular CDC25B blocked oncogenic AKT activation by rapamycin and enhanced the anticancer effect of rapamycin. Interestingly, we also discovered that a large percentage of the rapamycin-regulated proteins are involved in regulation of cellular transcription. These results show that rapamycin phosphoproteomics enables us to improve mTOR-targeted therapies, as well as advance the general mechanistic comprehension of rapamycin treatment in cancer.

Materials and Methods

Materials. The human cell lines HeLa, MCF-7, and Du145 were obtained from American Type Culture Collection. The human H157 was kindly provided by Dr. Shi-Yong Sun (Winship Cancer Institute, Emory University School of Medicine, Atlanta, Georgia). All cells were cultured in DMEM with 5% fetal bovine serum (FBS), 1% penicillin/streptomycin, and 1% L-glutamine (Invitrogen). Anti–phospho-AKT (Ser473) antibody was from Upstate (Lake Placid). Anti–phospho-p38 (T180/Y182), p38, p-S6K1(T389), and p-eIF4E (S209) antibodies were from Cell Signaling. Anti–glyceraldehyde-3-phosphate dehydrogenase (GAPDH) antibody and rapamycin were from Calbiochem. Anti-CDC25B (C-20), anti-rabbit, and anti-mouse secondary antibodies were from Santa Cruz Biotechnology, Inc. Topflash reporter cells were kindly provided by Dr. Willert (University of California at San Diego, La Jolla, CA). pCRE-Luc reporter plasmid is from Stratagene.

Cell culture, SILAC-labeling, and sample preparation for mass spectrometry. Life Technologies SILAC DMEM basal cell culture medium

Note: Supplementary data for this article are available at Cancer Research Online (http://cancerres.aacrjournals.org/).

R-q. Chen, Q-k. Yang, B-w. Lu, W. Yi, and G. Cantin contributed equally.

Requests for reprints: Jiing-Dwan Lee or John R. Yates III, The Scripps Research Institute, IMM-12, 10550 North Torrey Pines Road, La Jolla, CA 92037. Phone: 858-784-8703; Fax: 858-784-8343; E-mail: jdlee@scripps.edu or jyates@scripps.edu.

doi:10.1158/0008-5472.CAN-08-3222

Published OnlineFirst March 10, 2009; DOI: 10.1158/0008-5472.CAN-08-3222

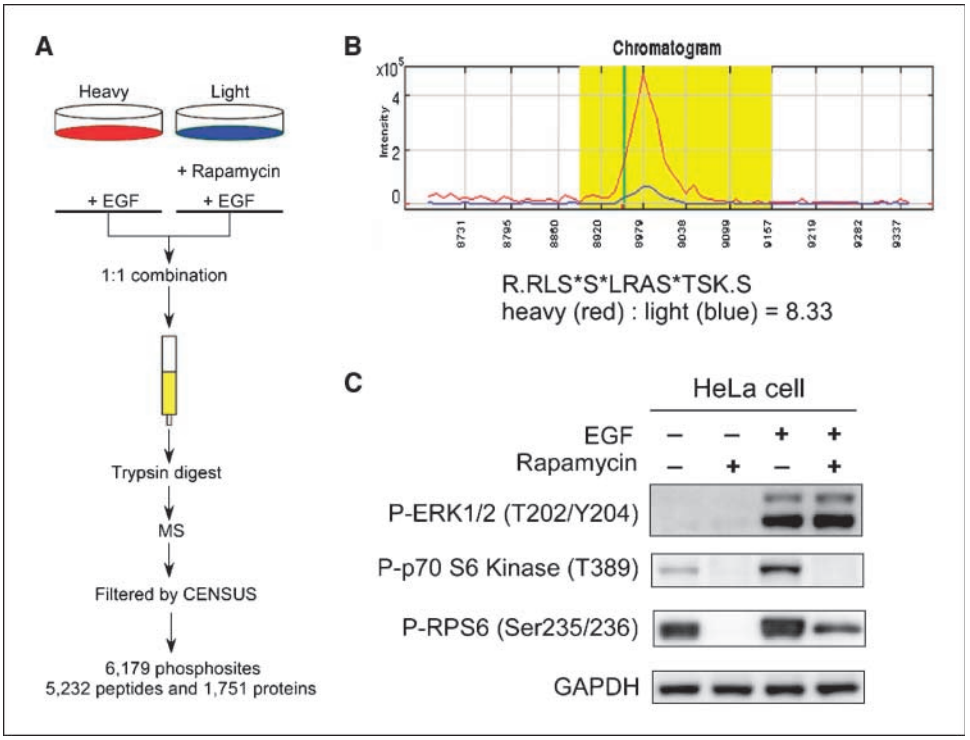

Figure 1. Experimental design for rapamycin-dependent phosphoproteomic profiling. *A,* Heavy cells were pretreated with 25 nmol/L rapamycin for 1 h followed by 15 min treatment with 10 ng/mL EGF. Light cells were only treated with 10 ng/mL EGF for 15 min. Heavy and light cell lysates were combined in a 1:1 ratio. Phosphorylation of each peptide was quantified by measuring the peak area of light and heavy peptides in the MS spectra with the CENSUS program. A total of 6,179 phosphosites was detected. *B,* a chromatogram of heavy and light phosphopeptides of RPS6 (R.RLS*S*LRAS*TSK.S), showing a rapamycin-dependent 8.33-fold inhibition by area ratio. *Red line,* heavy phosphopeptide treated with EGF; *blue line,* light phosphopeptide treated with EGF and rapamycin. *C,* Western blot analysis of cell lysates showing modification of the phosphorylation of ERK1/2, p70S6K, and RPS6 proteins by the indicated treatment, using anti–phospho-p70S6K (S389), anti–phospho-ERK1/2 (T202/Y204), and anti–phospho-RPS6 S235/S236 antibodies. GAPDH was used as loading control.

(Invitrogen) containing 2 mmol/L L-Glutamine, 10% dialyzed FBS (Invitrogen), and 100 U/mL penicillin and streptomycin was supplemented with 100 mg/L L-Lysine and 20 mg/L L-Arginine, or 100 mg/L [U-$^{13}C_6$]-L-Lysine and 20 mg/L [U-$^{13}C_6$, $^{15}N_4$]-L-Arginine (Invitrogen) to make the "Light" SILAC or "Heavy" SILAC culture medium respectively. HeLa cells were obtained from American Type Culture Collection and were propagated in SILAC medium for >9 generations to ensure nearly 100% incorporation of labeled amino acids before the experiment was performed. Before cell treatment, both heavy- and light-labeled cells were cultured overnight in the corresponding SILAC medium without FBS. "Heavy" cells were treated for 15 min with epidermal growth factor (EGF; R&D Systems). "Light" cells were pretreated with rapamycin for 1 h followed by addition of EGF. After being washed with cold PBS buffer, HeLa cells were harvested and lysed in an Extraction/Loading buffer from the TALON PMAC Phosphoprotein Enrichment kit (Clontech) supplemented with 10 mmol/L sodium fluoride and a cocktail of protease inhibitors (Roche). Light cell lysate and Heavy lysates were mixed at 1:1 ratio, and 16 mg of the mixed lysate was loaded equally onto two phosphoprotein affinity columns (Talon PMAC; Clontech) following the manual. The eluate was reduced with DTT and then alkylated with iodoacetamide. The resulting solution was dialyzed against 1 mol/L urea/100 mmol/L NH_4HCO_3 at 4°C overnight. The samples were digested with trypsin (Promega). The digestion was subjected to solid phase extraction by Extract-clean SPE C18 column (Alltech Associates) and later lyophilized. The lyophilized peptide sample was loaded onto four IMAC spin columns (Pierce Biotechnology). The IMAC-retained peptides were then washed and eluted as recommended by the manufacturer's manual. Formic acid was added to the phosphopeptide-enriched eluate to a final concentration of 4%, and the eluate was subsequently centrifuged to remove any particulate matter before analysis by MudPIT(16).

Purified phosphopeptide samples were centrifuged to remove any particulate matter before being analyzed by tandem mass spectrometry (MS/MS) using an online high performance liquid chromatography system (Nano LC-2D; Eksigent) coupled with a hybrid LTQ Orbitrap mass spectrometer (Thermo Electron). The LC/LC and MS/MS were performed as previously described (15).

Acquired MS/MS and MS/MS/MS spectra were subjected to SEQUEST searches against the EBI-IPI human database (version 3.17 released 05-09-2006) attached with common contaminants (e.g., proteases and keratins) with its reverse decoy for the assessment of false positive rates. Phosphorylation searches were performed where serine, threonine, and tyrosine were allowed to be differentially modified as previous described (15). The SEQUEST identifications were additionally filtered using a false positive cutoff by the DTASelect program based on XCorr and DeltaCN scores using a reversed database approach (17). All identified phosphopeptides were subjected to relative quantification analysis using the program Census (18). The Census program quantifies relative abundances of light and heavy versions of precursor peptides identified by MS/MS and/or MS/MS/MS spectra. The R-square statistics were calculated by regression analysis of the profile of the heavy-peptide and the profile of the light-peptide using the Census program. A *P* value for each phosphopeptide ratio was calculated according to the distribution of peptide ratio measurements of the 1:1 heavy/light mixed lysates.

siRNA-dependent function screen. Eighteen rapamycin-sensitive kinases and phosphatases were screened for their ability to mediate AKT activation by rapamycin. HeLa cells were individually transfected with siRNAs (Dharmacon) of these kinases and phosphatases. After 72 h, these cells were treated with 100 nmol/L rapamycin for 3 h. Western blot was used to detect phosphorylation changes in AKT at Ser-473.

Phosphatase assays. Expression plasmid encoding Myc-tagged CDC25B (a gift from Dr. Brian Gabrielli, University of Queensland, Queensland, Australia) was transfected into HEK293 cells. After 48 h, CDC25B protein was immunoprecipitated using anti-Myc antibody. These immunoprecipitates were incubated with 300 μmol/L 3-O-methyl fluorescein phosphate (Sigma) in 50 mmol/L Tris-HCl (pH 8.2), 50 mmol/L NaCl, 1 mmol/L DTT, and 20% glycerol for 15 min at 30°C. Hydrolysis of 3-O-methyl fluorescein phosphate to OMF was monitored at 477 nm.

Dual luciferase assay. HeLa cells were plated in 24-well plates in DMEM containing 2 mmol/L L-Glutamine and 10% FBS. Cells were cotransfected with various promoter-firefly luciferase reporters (200 ng DNA per well) and pRL-TK reporter (20 ng DNA per well) using GeneJet DNA *In Vitro* Transfection reagent (SignaGen Laboratories) following the manufacturer's protocol. After 24 h, cells were changed to serum-free medium and treated with indicated reagents. The resultant cells were lysed and analyzed for luciferase activity using the dual luciferase assay (Promega) according

Published OnlineFirst March 10, 2009; DOI: 10.1158/0008-5472.CAN-08-3222

to the manufacturer's instruction. All experiments were repeated at least thrice with similar results.

Results

Rapamycin phosphoproteome generation and results. Rapamycin inhibits the ability of mTOR protein kinase to phosphorylate cellular proteins, thereby blocking the cancerous signals derived from mTOR. Therefore, to profile rapamycin-modulated cellular proteins, we compare the phosphoproteome of two growth factor induced–cell cultures pretreated with or without rapamycin. Briefly, cells in normal medium (light culture) were treated with rapamycin, and cells grown in medium containing stable isotopes (heavy culture) were treated with vehicle. These two populations of cells were stimulated with growth factor for 15 minutes, after which the 2 populations of cells were harvested, mixed at a 1:1 ratio, and subjected to double IMAC purifications followed by MudPIT LC/MS/MS analysis (15). Peptide sequences were obtained from the MS/MS and MS/MS/MS spectra by SEQUEST software. Phosphopeptides were obtained by filtering total peptides by DTASelect 2.0 using the default settings, followed by quantifying the abundance (peak area) of the light and heavy phosphopeptides by CENSUS 1.05 using the default filter setting. We detected 6,179 phosphosites derived from 1,751 phosphoproteins (Fig. 1*A*). As an example that this phosphoproteomic profiling succeeded, the phosphorylation of ribosomal protein S6 (RPS6) at S235 and S236 is controlled by mTOR and inhibited by rapamycin (19). Our rapamycin phosphoproteome data showed that a phosphopeptide from RPS6 was phosphorylated at S235, S236, and S240 and the phosphorylation was inhibited 8.33-fold by rapamycin (Fig. 1*B*). This was verified by Western blotting using an antiphospho RPS6 antibody (Fig. 1*C*).

To quantify the phosphorylation change for each phosphopeptide, we used the Census software to calculate area ratio, defined as the ratio of the "light" peak area over the "heavy" peak area in the chromatogram (Fig. 1*B*). An R-square statistic was provided to indicate the accuracy of each area ratio measurement (Supplementary Table S1). The 1:1 mixed unenriched lysates were analyzed by LC/LC-MS/MS to measure ratios of heavy and light peptides. The distribution of the log ratios of base 2 of this 1:1 mixture was studied. The mean of the log 2 ratios is −0.0892, and SD is 0.2546. Based on this distribution, the 2-σ cutoffs are log 2 ratio > 0.4200 or log 2 ratio < −0.5984, corresponding to ratios of >1.34 and <0.66, respectively. Because we believe that phosphopeptides more differentially expressed would also be more biologically interesting, we chose to use a more stringent 2-fold cutoff. Using >2 or <0.5 as the threshold for area ratio, we found that the phosphorylation of 250 sites (161 proteins) of 6,179 sites (1,751 proteins) was significantly modulated by rapamycin (Fig. 2*A* and *B*). In other words, only ~4% of the total phosphosites detected showed significant alteration after rapamycin treatment. Among these 250 rapamycin-sensitive phosphosites, only 3 have been reported previously as downstream targets of mTOR (Fig. 2*B*; ref. 19).

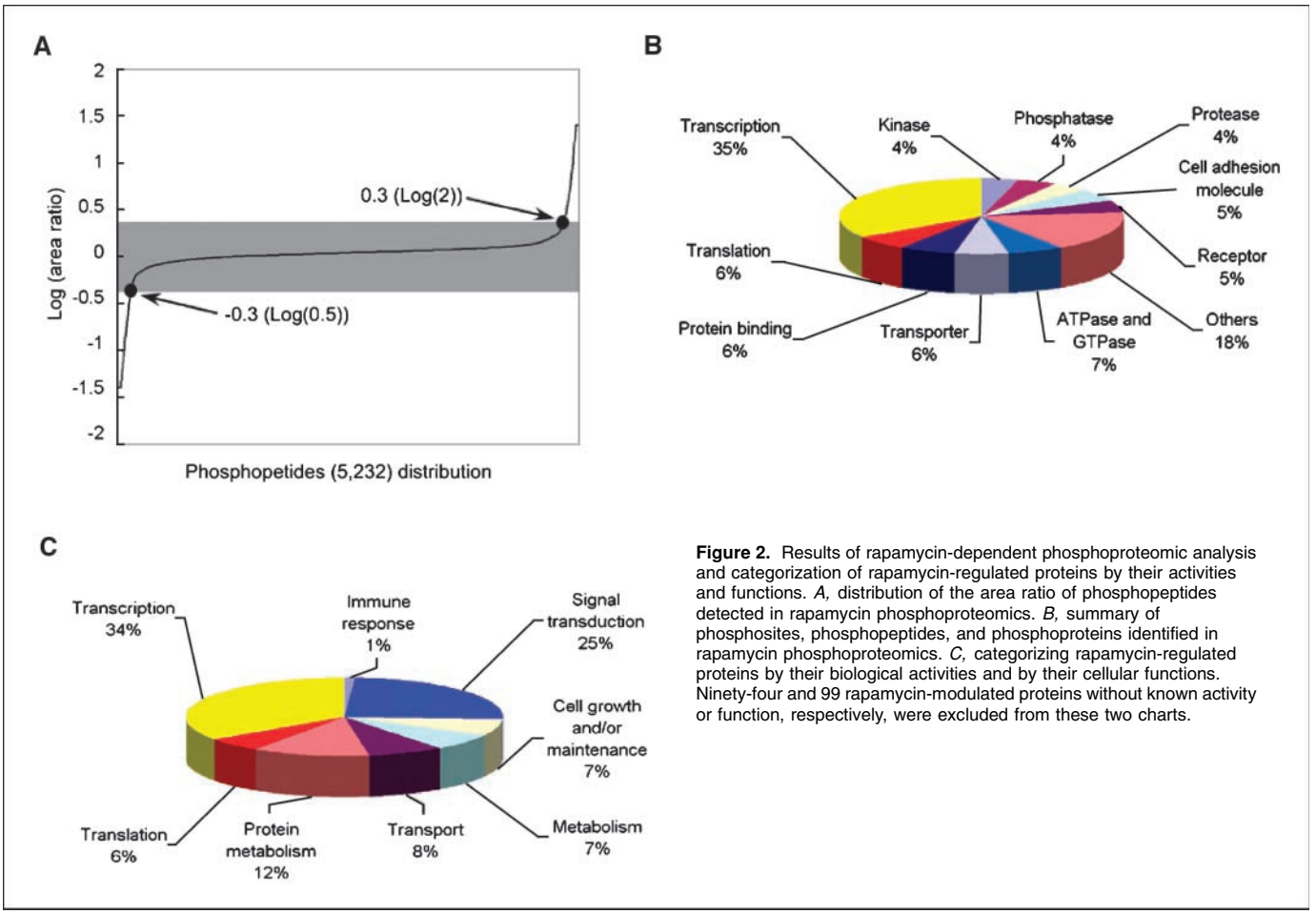

Figure 2. Results of rapamycin-dependent phosphoproteomic analysis and categorization of rapamycin-regulated proteins by their activities and functions. *A,* distribution of the area ratio of phosphopeptides detected in rapamycin phosphoproteomics. *B,* summary of phosphosites, phosphopeptides, and phosphoproteins identified in rapamycin phosphoproteomics. *C,* categorizing rapamycin-regulated proteins by their biological activities and by their cellular functions. Ninety-four and 99 rapamycin-modulated proteins without known activity or function, respectively, were excluded from these two charts.

Published OnlineFirst March 10, 2009; DOI: 10.1158/0008-5472.CAN-08-3222

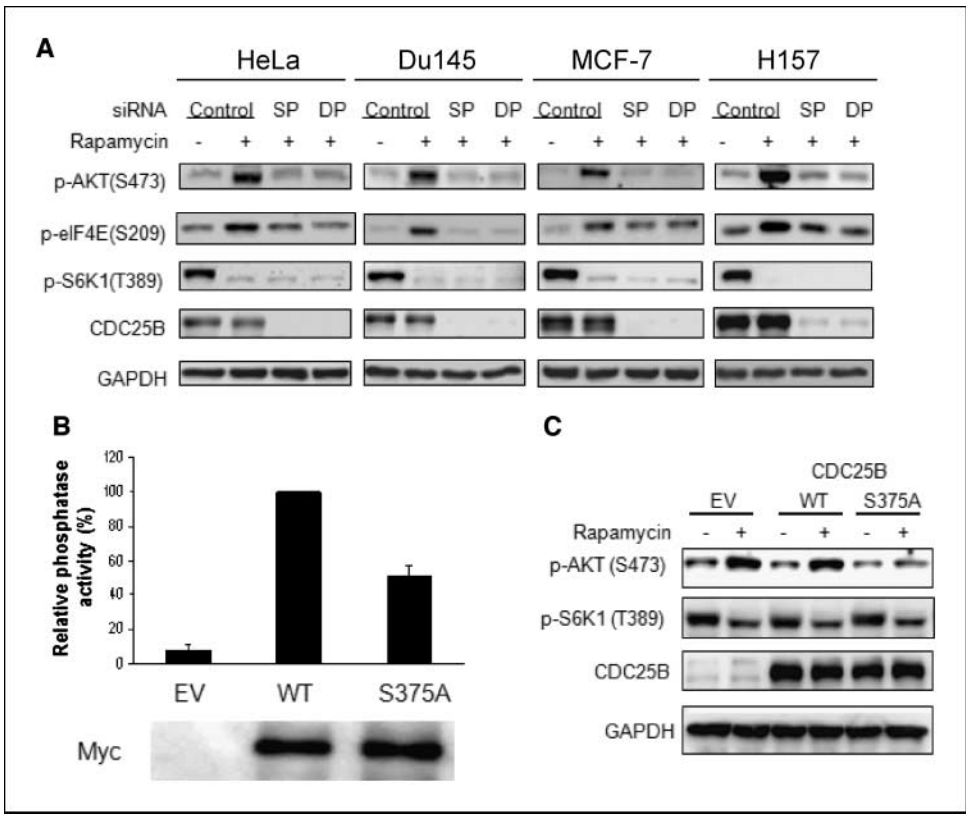

Figure 3. CDC25B mediates activation of the oncogenic AKT pathway by rapamycin. *A,* effect of CDC25B depletion on AKT activation by rapamycin in cancer cell lines. Cells were transfected with CDC25B-specific smartpool siRNA (*SP*), duplex siRNAs (*DP*), or control siRNAs for 60 h. Cells were then treated with 100 nmol/L rapamycin for 3 h. The phosphorylation of AKT(S473), eIF4E (S209), S6K1(T389), and expression of CDC25B and GAPDH proteins were detected by immunoblotting. *B,* HEK293 cells were transfected with empty vector (*EV*) or expression plasmids encoding Myc-tagged WT or mutant CDC25B with its Serine 375 mutated to Ala (*S375A*). Forty-eight hours posttransfection, cells were collected and phosphatase activities of empty vector, WT, and S375A were assessed as described in Materials and Methods. Relative phosphatase activity in these cells was normalized using WT-transfected cells whose value was taken as 100%. *C,* empty vector or expression plasmids encoding WT or mutant CDC25B, CDC25B (S375A), were transfected into cells, followed by 100 nmol/L rapamycin stimulation. The phosphorylation of AKT(S473), S6K1(T389), and expression of CDC25B and GAPDH proteins were detected by immunoblotting.

Categorizing rapamycin-regulated proteins by their activities and functions. To perceive the scope of rapamycin action in cancer cells, we used the human protein reference database to classify the 161 rapamycin-sensitive proteins by their cellular activities and functions (Fig. 2*C* and *D*). Previous studies indicated that rapamycin exerts its anticancer function by inhibiting protein translation in cancer cells (20). Interestingly, in our screen, the largest percentage (35%) of the rapamycin-regulated proteins was involved in regulation of transcription and not translation (6%; Fig. 2*C*). Additional examination showed that 32 of 345 (9.3%) transcription-related proteins and 6 of 112 (5.4%) translation-related proteins detected in phosphoproteomic analysis with their phosphorylation significantly altered by rapamycin (Supplementary Table S1). Thus, rapamcyin has significant effect on 9.3% of transcription regulators detected versus 5.4% of translational regulators detected. These data suggested that the cancer-inhibitory effect of rapamycin may also rely on its regulatory role in mRNA transcription.

CDC25B mediates the activation by rapamycin of the oncogenic Akt pathway. Kinases and phosphatases are critical signal mediators and, thus, excellent cancer drug targets. We found that rapamycin modulates four kinases and four phosphatases (Fig. 2*C*) and suspected that these kinases/phosphatases may transduce the oncogenic signal induced by rapamycin. We screened these kinases/phosphatases for their ability to mediate rapamycin-induced AKT and elF4E activation. We found that silencing CDC25B phosphatase blocked the activation of AKT and eIF4E by rapamycin in various human tumor cell lines (Fig. 3*A*). Rapamycin induced phosphorylation of CDC25B at Serine 375 (Supplementary Table S1). To examine the effect of this phosphorylation on the phosphatase activity of CDC25B, we expressed either wild-type (WT) or a mutant form of CDC25B [CDC25B (S375A)] in cells and subsequently analyzed their phosphatase activity. We found that mutation of Serine 375 to Alanine in CDC25B significantly attenuate its phosphatase activity (Fig. 3*B*). We next expressed this CDC25B mutant in cells followed by rapamycin treatment and found that CDC25B (S375A) effectively blocked AKT activation by rapamycin, whereas WT CDC25B did not (Fig. 3*C*). In UV-induced DNA damage, p38 is the upstream regulatory kinase for CDC25B (21). However, silencing of p38 did not affect the activation of AKT by rapamycin (Fig. 4*A*). Instead, surprisingly, CDC25B knockdown blocked p38 activation by rapamycin (Fig. 4*B*), indicating that p38 is downstream of CDC25B in the activation of AKT. As blocking CDC25B inhibits the activation of the oncogenic pathways, AKT and elF4E, by

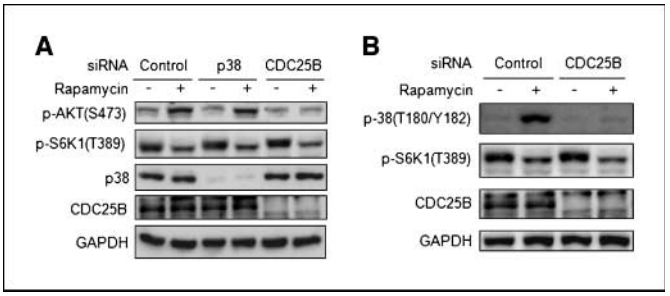

Figure 4. CDC25B mediates activation of the p38 mitogen-activated protein kinase by rapamycin. *A,* depletion of cellular p38 has no effect in AKT activation by rapamycin. Cells were transfected for 60 h with p38-specific, CDC25B-specific, or control siRNAs as indicated, before being treated with 100 nmol/L rapamycin for 15 min. Phosphorylation of AKT, S6K1, p38, and CDC25B was detected by immunoblotting. GAPDH protein was used as loading control. *B,* CDC25B depletion attenuated p38 activation by rapamycin. Cells were transfected with CDC25B-specific siRNA or control siRNA for 60 h before treatment with 100 nmol/L rapamycin for 15 min. Phosphorylation of p38 (T180/Y182), S6K1 (T389), and expression of CDC25B were detected by immunoblotting.

Published OnlineFirst March 10, 2009; DOI: 10.1158/0008-5472.CAN-08-3222

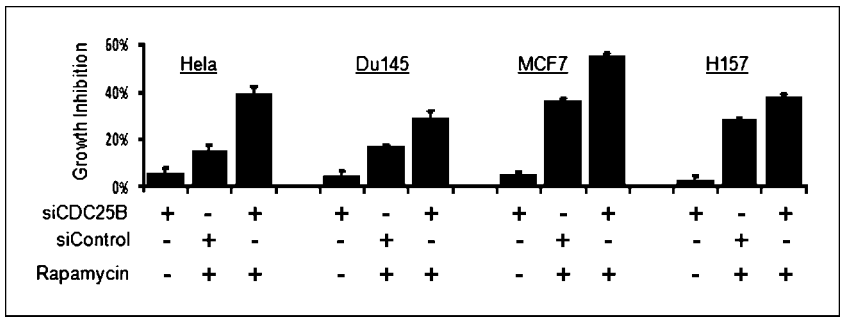

Figure 5. Cellular depletion of CDC25B enhances the anticancer effect of rapamycin. CDC25B depletion enhanced the growth-inhibitory effect of rapamycin in different cancer cell lines. Cells were transfected with CDC25B-specific siRNAs or control siRNAs for 24 h followed by treatment with 100 nmol/L rapamycin for another 48 h as indicated. Viable cell count was estimated by the 3-(4,5-dimethylthiazol-2-yl)-2,5-diphenyltetrazolium bromide (MTT) assay. % Growth inhibition was calculated relative to the MTT value from cells transfected with control siRNA only.

rapamycin, we hypothesized that CDC25B knockdown in tumor cells should enhance the anticancer effects of rapamycin. To test this, in the presence or absence of rapamycin, we knocked down CDC25B in various types of cancer cells containing genetic mutations (Supplementary Table S2) that augment or deregulate the mTOR pathway. Moreover, as anti-mTOR treatment is only effective in few types of human cancer (e.g., kidney cancer and mantle B cell; ref. 13), we want to test whether our finding may help enhancing the anti-mTOR treatment of some other kinds of cancers such as prostate (Du145), breast (MCF7), non–small cell lung (H157), and cervical (HeLa) cancers. We found that CDC25B knockdown enhanced the antiproliferative effect of rapamycin on cancer cells by 0.5- to 2.5-fold (Fig. 5). Furthermore, CDC25B silencing only additively but not synergistically enhanced cell cycle effect by rapamycin (Supplementary Fig. S1). These data suggest that CDC25B mediates the rapamycin-induced activation of AKT, elF4E, and p38 cascades, and CDC25B knockdown significantly promotes the inhibitory effect of rapamycin on the growth of cancer cells not only through blocking cell cycle progression but also by inhibiting oncogenic pathways activation by rapamycin.

Discussion

The CDC25 family of proteins is comprised of dual specificity phosphatases that regulate cell cycle transitions, and are key targets of the checkpoint machinery to maintain genome stability (22) during DNA damage. Three isoforms of CDC25 have been identified in mammalian cells: CDC25A, CDC25B, and CDC25C. CDC25A and CDC25B overexpression has been reported in many types of human cancers (22, 23) but is insufficient to cause cancer (22), and the mechanism responsible for CDC25 overexpression is unclear. Nevertheless, CDC25A and CDC25B overexpression correlates with aggressive, high-grade, and late-stage tumors (22), as well as with a poor prognosis for cancer patients (22, 24, 25), possibly resulting from genome instability caused by the checkpoint-abrogating effect of their overexpression. However, CDC25 may contribute to tumorigenesis by other mechanism(s). Herein, we discovered that the anticancer drug, rapamycin, induced the phosphorylation of CDC25B at Serine 375, which is critical for its phosphatase activity, and depletion of cellular CDC25B inhibited the rapamycin-dependent activation of the survival/oncogenic AKT, elF4E, and p38 pathways, suggesting that CDC25B phosphatase activity is required for the activation of Akt and/or p38. It is possible that CDC25B might dephosphorylate and subsequently activate the upstream regulator(s) of AKT and/or p38 but the exact mechanism for this needs further investigation. Moreover, the depletion of cellular CDC25B resulted in the augmentation of anticancer effect of rapamycin on various types of tumor cells. This result indicates that CDC25B is the key mediator for supplying survival/oncogenic signals to tumor cells during mTOR-targeted cancer treatment and provide us with a potential drug target to improve the efficacy of anticancer drugs rapamycin and its derivatives.

It is well-known that the mTOR/Raptor (rapamycin-sensitive) pathway is critical in modulating cellular translational machineries thereby regulating physiologic and pathologic responses in cell. However, the role of this pathway in altering cellular transcription apparatuses has been emphasized much less. Interestingly, 35% of the mTOR/Raptor-regulated cellular proteins identified herein are transcriptional factors/transcription regulators and only 6% are proteins controlling cellular translation processes (Fig. 2*C*). Further analysis showed that 32 of 345 (9.3%) transcription-related proteins and 6 of 112 (5.4%) translation-related proteins detected in phosphoproteomic profiling have their phosphorylation levels significantly altered by rapamycin (Supplementary Table S1). It seems that the effect of the mTOR/Rapamycin pathway in altering mRNA transcription and the consequent effect on gene expression, biological function, and disease progression may has been underestimated. Further studies to clarify molecular mechanisms and identify key cellular mediator(s) for these rapamycin-induced phosphorylation alterations of transcription regulators should facilitate the development of approaches to improve the efficacy or reduce unwanted side effects during the mTOR-targeted cancer therapies.

In conclusion, using rapamycin phosphoproteomics, we identified hundreds of novel rapamycin-targeted cellular proteins and their phosphorylation sites. This information enabled us to identify CDC25B as the key enzyme in mediating rapamycin induced oncogenic AKT activation. Importantly, we show that phosphoproteomic profiling of a certain therapeutic agent cannot only identify potential drug target(s) to improve the efficacy of that therapeutic approach in disease treatment but also provide cellular information of possible beneficial and adverse side effects of a certain disease therapy when treating patients.

Disclosure of Potential Conflicts of Interest

No potential conflicts of interest were disclosed.

Acknowledgments

Received 8/20/2008; revised 12/29/2008; accepted 1/9/2009; published OnlineFirst 3/10/09.

Grant support: NIH, CA079871 and CA114059 (J.-D. Lee). This research was supported by funds from the Tobacco-Related Disease, Research Program of the University of California, 15RT-0104 (J.-D. Lee).

The costs of publication of this article were defrayed in part by the payment of page charges. This article must therefore be hereby marked *advertisement* in accordance with 18 U.S.C. Section 1734 solely to indicate this fact.

We thank Dr. Albert J. Fornace, Jr. (National Cancer Institute, Bethesda, MD) for CDC25B plasmids.

Published OnlineFirst March 10, 2009; DOI: 10.1158/0008-5472.CAN-08-3222

References

1. Bjornsti MA, Houghton PJ. The TOR pathway: a target for cancer therapy. Nat Rev Cancer 2004;4:335–48.
2. Sawyers CL. Will mTOR inhibitors make it as cancer drugs? Cancer Cell 2003;4:343–8.
3. Hay N, Sonenberg N. Upstream and downstream of mTOR. Genes Dev 2004;18:1926–45.
4. Easton JB, Houghton PJ. mTOR and cancer therapy. Oncogene 2006;25:6436–46.
5. Rampaul RS, Pinder SE, Gullick WJ, Robertson JF, Ellis IO. HER-2 in breast cancer-methods of detection, clinical significance and future prospects for treatment. Crit Rev Oncol Hematol 2002;43:231–44.
6. Li SY, Rong M, Grieu F, Iacopetta B. PIK3CA mutations in breast cancer are associated with poor outcome. Breast Cancer Res Treat 2006;96:91–5.
7. Depowski PL, Rosenthal SI, Ross JS. Loss of expression of the PTEN gene protein product is associated with poor outcome in breast cancer. Mod Pathol 2001;14:672–6.
8. Koksal IT, Dirice E, Yasar D, et al. The assessment of PTEN tumor suppressor gene in combination with Gleason scoring and serum PSA to evaluate progression of prostate carcinoma. Urol Oncol 2004;22:307–12.
9. Pfeil K, Eder IE, Putz T, et al. Long-term androgen-ablation causes increased resistance to PI3K/Akt pathway inhibition in prostate cancer cells. Prostate 2004;58:259–68.
10. Edwards J, Krishna NS, Witton CJ, Bartlett JM. Gene amplifications associated with the development of hormone-resistant prostate cancer. Clin Cancer Res 2003;9:5271–81.
11. McMenamin ME, Soung P, Perera S, Kaplan I, Loda M, Sellers WR. Loss of PTEN expression in paraffin-embedded primary prostate cancer correlates with high Gleason score and advanced stage. Cancer Res 1999;59:4291–6.
12. Graff JR, Konicek BW, McNulty AM, et al. Increased AKT activity contributes to prostate cancer progression by dramatically accelerating prostate tumor growth and diminishing p27Kip1 expression. J Biol Chem 2000;275:24500–5.
13. Faivre S, Kroemer G, Raymond E. Current development of mTOR inhibitors as anticancer agents. Nat Rev Drug Discov 2006;5:671–88.
14. Sun SY, Rosenberg LM, Wang X, et al. Activation of Akt and eIF4E survival pathways by rapamycin-mediated mammalian target of rapamycin inhibition. Cancer Res 2005;65:7052–8.
15. Cantin GT, Yi W, Lu B, et al. Combining protein-based IMAC, peptide-based IMAC, and MudPIT for efficient phosphoproteomic analysis. J Proteome Res 2008;7:1346–51.
16. Washburn, MP, Wolters D, Yates JR III. Large-scale analysis of the yeast proteome by multidimensional protein identification technology. Nat Biotechnol 2001;19:242–7.
17. Peng J, Elias JE, Thoreen CC, Licklider LJ, Gygi SP. Evaluation of multidimensional chromatography coupled with tandem mass spectrometry (LC/LC-MS/MS) for large-scale protein analysis: the yeast proteome. J Proteome Res 2003;2:43–50.
18. Park SK, Venable JD, Xu T, Yates JR III. A quantitative analysis software tool for mass spectrometry-based proteomics. Nat Methods 2008;5:319–22.
19. Chiu T, Santiskulvong C, Rozengurt E. EGF receptor transactivation mediates ANG II-stimulated mitogenesis in intestinal epithelial cells through the PI3-kinase/Akt/mTOR/p70S6K1 signaling pathway. Am J Physiol Gastrointest Liver Physiol 2005;288:G182–94.
20. Hidalgo M, Rowinsky EK. The rapamycin-sensitive signal transduction pathway as a target for cancer therapy. Oncogene 2000;19:6680–6.
21. Bulavin DV, Higashimoto Y, Popoff IJ, et al. Initiation of a G2/M checkpoint after ultraviolet radiation requires p38 kinase. Nature 2001;411:102–7.
22. Boutros R, Lobjois V, Ducommun B. CDC25 phosphatases in cancer cells: key players? Good targets? Nat Rev Cancer 2007;7:495–507.
23. Galaktionov K, Lee AK, Eckstein J, et al. CDC25 phosphatases as potential human oncogenes. Science 1995;269:1575–7.
24. Ito Y, Yoshida H, Tomoda C, et al. A. Expression of cdc25B and cdc25A in medullary thyroid carcinoma: cdc25B expression level predicts a poor prognosis. Cancer Lett 2005;229:291–7.
25. Takemasa I, Yamamoto H, Sekimoto M, et al. Overexpression of CDC25B phosphatase as a novel marker of poor prognosis of human colorectal carcinoma. Cancer Res 2000;60:3043–50.

Cancer Research
The Journal of Cancer Research (1916–1930) | The American Journal of Cancer (1931–1940)

AACR American Association for Cancer Research

CDC25B Mediates Rapamycin-Induced Oncogenic Responses in Cancer Cells

Run-qiang Chen, Qing-kai Yang, Bing-wen Lu, et al.

Cancer Res 2009;69:2663-2668. Published OnlineFirst March 10, 2009.